GEOPHYSICAL RESEARCH LETTERS, VOL. 33, L15304, doi:10.1029/2006GL026348, 2006

$NaMgF_3$: A low-pressure analog of $MgSiO_3$

K. Umemoto,[1] R. M. Wentzcovitch,[1] D. J. Weidner,[2] and J. B. Parise[2]

Received 19 March 2006; revised 14 June 2006; accepted 21 June 2006; published 3 August 2006.

[1] Using first principles computations we show that $NaMgF_3$ perovskite undergoes the same series of phase transitions as $MgSiO_3$ perovskite, that is, the post-perovskite transition and the dissociation into CsCl-type NaF and cotunnite-type MgF_2. These fluorides also undergo the same series of phase transitions as MgO and SiO_2, the dissociation products of $MgSiO_3$. Since the phase transformations in $NaMgF_3$ are not accompanied by any soft mode, we compute quasi-harmonic free energies and the respective phase boundaries. They have positive and negative Clapeyron slopes, respectively, like $MgSiO_3$. However, the transition pressures in $NaMgF_3$ are much lower and could be easily achieved in diamond anvil experiments. Therefore $NaMgF_3$ should be a good low-pressure analog of $MgSiO_3$. **Citation:** Umemoto, K., R. M. Wentzcovitch, D. J. Weidner, and J. B. Parise (2006), $NaMgF_3$: A low-pressure analog of $MgSiO_3$, *Geophys. Res. Lett.*, *33*, L15304, doi:10.1029/2006GL026348.

1. Introduction

[2] Since the discovery of the transition from perovskite (PV) to $CaIrO_3$-type post-perovskite (PPV) phase in $MgSiO_3$ near the core-mantle boundary of the Earth (at ~125 GPa and 2500 K) [*Murakami et al.*, 2004; *Tsuchiya et al.*, 2004; *Oganov and Ono*, 2004], this transition has been attracting great interest. Very recently we have predicted the dissociation of $MgSiO_3$ PPV into CsCl-type MgO and cotunnite-type SiO_2 at ultrahigh pressure and temperature (PT) typical of solar giants, Jupiter and Saturn, and newly-found extrasolar planets [*Umemoto et al.*, 2006]. Unfortunately, the predicted dissociation pressure is too high (~1 TPa) to be achieved experimentally today. Therefore low-pressure analogs of $MgSiO_3$ are highly desired for experimental investigation of properties of the $CaIrO_3$-type structure. $NaMgF_3$ PV, neighborite, is one of the best candidates. It is a stable *Pbnm* perovskite phase at ambient condition and undergoes a transition to a cubic phase by elevating temperature. The temperature dependence of structural parameters has been studied in detail [*Zhao et al.*, 1993a, 1993b, 1994; *Zhou et al.*, 1997; *Smith et al.*, 2000]. The PPV transition occurs also in $NaMgF_3$ under pressure [*Parise et al.*, 2004; *Liu et al.*, 2005]. However, the pressure dependence of $NaMgF_3$'s structural properties has been reported in detail only at low pressure [*Zhao et al.*, 1994], not near the PPV transition. If $NaMgF_3$ is a good low-pressure analog of $MgSiO_3$, then the ternary system of Na, Mg, and F could be useful for comparison at higher pressures as well. It would be particularly important for investigations of the $CaIrO_3$-type structure and its dissociation into the elementary fluorides NaF and MgF_2, which are also low-pressure analogs of MgO and SiO_2 [*Yagi et al.*, 1983; *Haines et al.*, 2001].

[3] In this paper, we investigate $NaMgF_3$ under pressure by first-principles and demonstrate that $NaMgF_3$ should undergo the same types of pressure-induced phase transitions as $MgSiO_3$: the transition from the PV to PPV phase and the dissociation of the PPV phase into CsCl-type NaF and cotunnite-type MgF_2.

2. Computational Method

[4] Calculations were performed using the local-density approximation (LDA) and the generalized-gradient approximation (GGA) [*Perdew and Zunger*, 1981; *Perdew et al.*, 1996]. The valence electronic configurations used for the generation of Vanderbilt ultrasoft pseudopotentials [*Vanderbilt*, 1990] are $2s^2\ 2p^6 3s^1\ 3p^0\ 3d^0$, $2s^2\ 2p^6\ 3s^2\ 3p^0\ 3d^0$, and $2s^2\ 2p^5\ 3d^0$, for Na, Mg, and F, respectively. Their cutoff radii are 1.6 a.u. for all quantum numbers l in each atom. The plane-wave cutoff energy is 60 Ry. We used variable-cell-shape molecular dynamics [*Wentzcovitch*,

Table 1. Calculated Parameters of the Third-Order Birch-Murnaghan Equations of States by LDA and GGA for Perovskite $NaMgF_3$, Post-Perovskite $NaMgF_3$, NaCl-type NaF, and Rutile-type MgF_2[a]

	V_0, a.u.^{3}/f.u.	B_0, GPa	B'_0
$NaMgF_3$ PV at 0 GPa			
Calc. (static)	358.07 (397.30)	86.9 (67.5)	3.7 (4.1)
Calc. (300 K)	366.98 (409.02)	80.1 (59.1)	3.8 (4.3)
Exp.[b]	380.27	67.6	
NaCl-type NaF at 0 GPa			
Calc. (static)	154.05 (175.20)	61.6 (45.1)	4.7 (4.5)
Calc. (300 K)	159.05 (182.31)	53.9 (37.9)	4.8 (4.7)
Exp.[c]	166.33	48.5	
Rutile-type MgF_2 at 0 GPa			
Calc. (static)	211.38 (230.55)	111.8 (90.4)	4.7 (4.6)
Calc. (300 K)	213.74 (234.57)	108.3 (83.4)	4.8 (4.6)
Exp.[d]	220.33	101	4.2
$NaMgF_3$ PPV at 0 GPa			
Calc. (static)	350.30 (391.47)	77.6 (60.8)	4.7 (4.5)
Calc. (300 K)	359.87 (403.75)	69.1 (54.6)	4.8 (4.5)

[a]The GGA results are in parentheses.
[b]At ambient temperature [*Zhao et al.*, 1994].
[c]At 300 K [*Cortona*, 1992].
[d]At ambient temperature [*Haines et al.*, 2001].

[1]Minnesota Supercomputing Institute and Department of Chemical Engineering and Materials Science, University of Minnesota, Minneapolis, Minnesota, USA.
[2]Department of Earth and Space Sciences, State University of New York, Stony Brook, New York, USA.

0094-8276/06/2006GL026348$05.00

Table 2. Calculated Transition Pressures by LDA and GGA for NaF and MgF_2[a]

	Static-calc.	300 K-calc.	Exp.
	NaF		
NaCl→CsCl	22.8 (27.1)	21.7 (26.0)	27[b]
	MgF_2		
Rutile→$CaCl_2$	5.8 (6.7)	7.5 (10.3)	9.1[c]
$CaCl_2$→Pyrite	9.0 (14.5)	8.6 (14.1)	14[c]
Pyrite→Cotunnite	33.5 (42.5)	32.9 (41.0)	36[c]

[a]The GGA results are shown in parentheses. The unit is GPa.
[b]At room temperature [*Yagi et al.*, 1983].
[c]At ambient temperature [*Haines et al.*, 2001].

1991; *Wentzcovitch et al.*, 1993] for structural optimization under arbitrary pressures. Dynamical matrices were computed at wave vectors **q** using density-functional perturbation theory [*Giannozzi et al.*, 1991; *Baroni et al.*, 2001]. The numbers of formula units in the unit cells, **k** points in the irreducible wedge, and **q** points are (4, 4, 8) for $NaMgF_3$ PV, (2, 6, 6) for $NaMgF_3$ PPV, (1, 10, 8) for NaCl-type NaF, (1, 20, 10) for CsCl-type NaF, (2, 6, 6) for rutile-type MgF_2, (2, 8, 8) for $CaCl_2$-type MgF_2, (4, 1, 4) for pyrite-type MgF_2, and (4, 2, 8) for cotunnite-type MgF_2. Force constants are extracted to build dynamical matrices at arbitrary phonon **q** vectors. Vibrational contributions to the free energy due to the zero-point motion (ZPM) and finite temperature are taken into account by the quasi-harmonic approximation (QHA) [*Wallace*, 1972].

[5] Comparisons between our calculated structural parameters (Table 1) and transition pressures (Table 2) with experimental values in Tables 1 and 2 confirm the reliability of our computational method. Notice that experimental data appear bracketed between LDA and GGA results, except the transition pressure from NaCl-type to CsCl-type NaF, where the experimental value is slightly larger than the GGA value but very close to it. Hence, the two series of calculations, one using the LDA and other the GGA should provide good predictions for the behavior of $NaMgF_3$ under pressure.

3. Results and Discussion

[6] Static LDA (GGA) enthalpy calculation shows $NaMgF_3$ PV transforms to PPV at 17.5 (22.5) GPa (blue line in Figure 1). Around the PPV transition pressure no phonon instability is found both in the PV and PPV phases, indicating that the PPV transition is enthalpically driven (Figure 2). At 0 GPa, all phonon frequencies in $NaMgF_3$ PPV are real and there is no dynamical instability. This is consistent with the experimental result that the PPV phase can be recovered at ambient pressure and room temperature [*Liu et al.*, 2005]. But imaginary phonon frequencies (soft mode) occur at negative pressure, ~−7 GPa (~−4 GPa) by LDA(GGA) (Figure 2). The lowest acoustic phonon branch along the Δ line goes soft entirely. Since this is a typical sign of amorphization, $NaMgF_3$ PPV should amorphize upon decompression at high temperatures (annealing), which is somewhat analogous to decompressing to negative pressures at 0 K.

[7] Next we investigate the dissociation of $NaMgF_3$ PPV into NaF and MgF_2. NaCl-type and CsCl-type NaF and pyrite-type and cotunnite-type MgF_2 are the relevant phases for the dissociation, because they are the stable phases beyond the PPV transition pressure (Table 2). Figure 1 shows that $NaMgF_3$ PPV dissociates into CsCl-type NaF and cotunnite-type MgF_2 at 40 GPa (LDA). The GGA dissociation pressure is 48 GPa. This dissociation pressure is much smaller than that of $MgSiO_3$ (~1 TPa) [*Umemoto et al.*, 2006] and can be easily achieved by diamond anvil experiments. There is no soft mode in CsCl-type NaF and cotunnite-type MgF_2 beyond the dissociation pressure and these phases are dynamically stable. $NaMgF_3$ PPV is also dynamically stable around the dissociation pressure; the dissociation as well as the PPV transition are enthalpically driven. Table 3 gives calculated structural parameters of $NaMgF_3$ PPV at 30 GPa and CsCl-type NaF and cotunnite-type MgF_2 at 50 GPa. They should be useful for the experimental identification of these phases.

[8] We have also investigated possible structures of post-PPV $NaMgF_3$: $LiSbO_3$-type $BaNiO_3$-type, hexagonal $BaTiO_3$-type, and $P6_3/mmc$ $NaMgF_3$. The former three structures are described by *Wyckoff* [1965] and *Hyde and Andersson* [1989]. The $LiSbO_3$-type structure consists of MgF_6 octahedra interconnected in an α-PbO_2-like network; this is a likely higher connectivity. In $BaNiO_3$-type structure, MgF_6 octahedra share their faces and form separate columns. In the hexagonal $BaTiO_3$-type structure, MgF_6 octahedra share their faces and apices. In these two structures, MgF_6 octahedra have a higher degree of connectivity than the PPV structure. The last $P6_3/mmc$ structure, to our knowledge, has not been observed experimentally so far. Its space group is a supergroup of *Cmcm*, the space group of the PPV structure. This structure has been found by a static compression of $NaMgF_3$ PPV to 150 GPa. Magnesium is 8-fold coordinated and the MgF_8 polyhedra share edges and apices. The MgF_8 network is related to Ni_2In-type structure. We found that all four phases have higher enthalpies than $NaMgF_3$ PPV around the dissociation pressure. At 50 GPa,

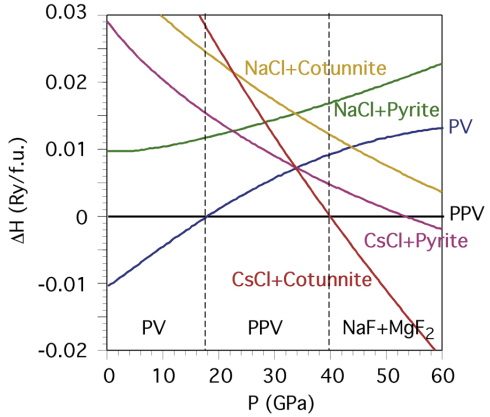

Figure 1. Pressure dependence of static-LDA enthalpies of $NaMgF_3$ PV and aggregations of NaF and MgF_2 with respect to $NaMgF_3$ PPV (ΔH).

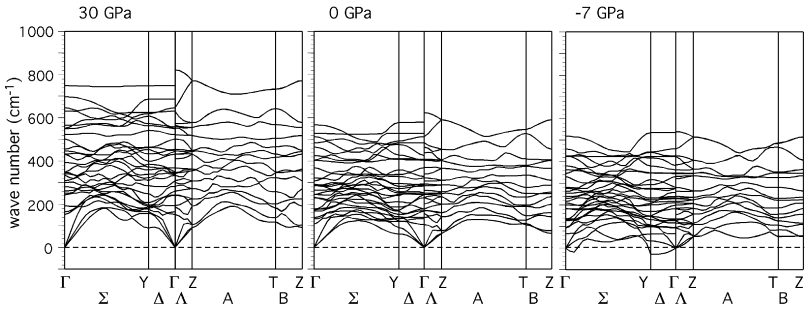

Figure 2. Phonon dispersion of $NaMgF_3$ PPV. Pressures are static-LDA values.

LDA calculations show that ΔH (Ry/f.u.) of these four structures with respect to $NaMgF_3$ PPV are 0.092, 0.173, 0.128, and 0.033, respectively.

[9] Using the QHA in conjunction with the computed phonon density of states (Figure 3), we obtain phase boundaries of the PPV transition and the dissociation (Figure 4). Empirically, the QHA works well below the temperature at which the thermal expansivity α (P, T) starts to deviate from linear behavior [*Karki et al.*, 1999]. Dashed lines in Figure 4 represent P-T conditions on which $d^2\alpha/dT^2 = 0$ for the investigated phases; the QHA should be valid at least up to these lines. The experimental PPV transition pressure at room temperature (19.7 GPa) [*Liu et al.*, 2005] is bracketed by LDA (19.4 GPa) and GGA (24.0 GPa) values at 300 K. The unit cell volume decreases through the PPV transition by ~2.5%. The shortest covalent Mg-F bond length also decreases through the transition by ~1%. These decreases induce higher phonon frequencies (Figure 3a) and consequently lower vibrational entropy in the PPV phase than those in the PV phase. Hence, ZPM energy increases the PPV transition pressure from the static value. The Clapeyron slope ($dP/dT = \Delta S/\Delta V$) of the PPV transition is positive, 6 (5) MPa/K at 500 K by LDA (GGA).

[10] Throughout the dissociation, the volume decreases by ~5–6%, while the covalent Mg-F bond length increases accompanied by an increase in the Mg coordination number (6 to 9). These longer covalent bonds give rise to smaller high (optical) phonon frequencies in general (Figure 3b). Hence, ZPM energy decreases the dissociation pressure from the static value. The Clapeyron slope is negative above ~300 K because of the overall increase in entropy: −1.7 (−1.8) MPa/K at 500 K and −3.3(−3.6) MPa/K at 1000 K by LDA (GGA). On the other hand, the volume shrinkage increases the lowest (acoustic) phonon frequencies (<~200–300 cm^{-1} ~300–400 K in Figure 3b). Since this effect compensates that of the longer bond lengths, the Clapeylon slope below ~300 K is almost independent on temperature. The same type of Clapeyron slope occurs in the transition of NaCl-type to CsCl-type NaF and pyrite-type to cotunnite-type MgF_2. In both cases there are increases in covalent bond lengths and cation coordination numbers and decrease of volumes.

[11] The present results show that $NaMgF_3$ PV undergoes the same sequence of phase transitions as $MgSiO_3$ PV: the PPV transition and the dissociation into NaF and MgF_2. The Clapeyron slopes of these transitions are positive and negative respectively, like the case of $MgSiO_3$. Transition pressures in $NaMgF_3$ are much smaller than those in $MgSiO_3$. Therefore, $NaMgF_3$ should be a good low-pressure analog of $MgSiO_3$ and serve as an alternative

Table 3. Calculated Lattice Constants and Atomic Wyckoff Positions of $NaMgF_3$ PPV at Static 30 GPa and CsCl-type NaF and Cotunnite-type MgF_2 at Static 50 GPa

	LDA	GGA
	$NaMgF_3$ PPV (Space Group: Cmcm)	
(*a*, *b*, *c*), a.u.	(5.238, 16.407, 12.995)	(5.343, 16.907, 13.240)
Na (4*c*)	(0, 0.252, 0.75)	(0, 0.252, 0.75)
Mg (4*a*)	(0, 0, 0)	(0, 0, 0)
F_1 (4*c*)	(0, 0.071, 0.25)	(0, 0.071, 0.25)
F_2 (8*f*)	(0, 0.360, 0.060)	(0, 0.362, 0.060)
	CsCl-type NaF (Space Group: Pm3m)	
a, a.u.	4.626	4.729
	Cotunnite-type MgF_2 (Space Group: Pbnm)	
(*a*, *b*, *c*), a.u.	(11.016, 9.377, 5.527)	(11.195, 9.547, 5.648)
Mg (4*c*)	(0.118, 0.248, 0.25)	(0.116, 0.249, 0.25)
F_1 (4*c*)	(0.429, 0.353, 0.25)	(0.428, 0.354, 0.25)
F_2 (4*c*)	(0.667, 0.978, 0.25)	(0.667, 0.979, 0.25)

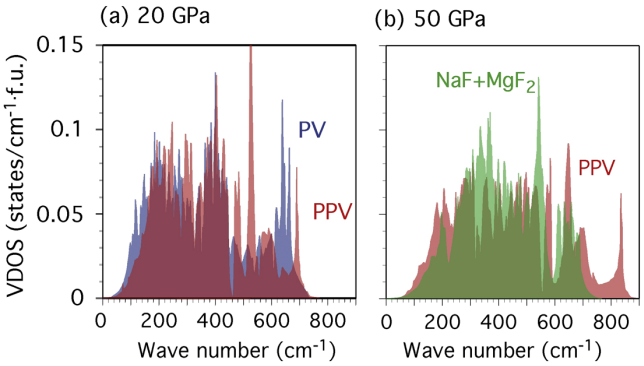

Figure 3. Vibrational density of states (VDOS) of (a) $NaMgF_3$ PV and PPV at 20 GPa and (b) $NaMgF_3$ PPV and aggregation of CsCl-type NaF and cotunnite-type MgF_2 at 50 GPa. Pressures are static-LDA values.

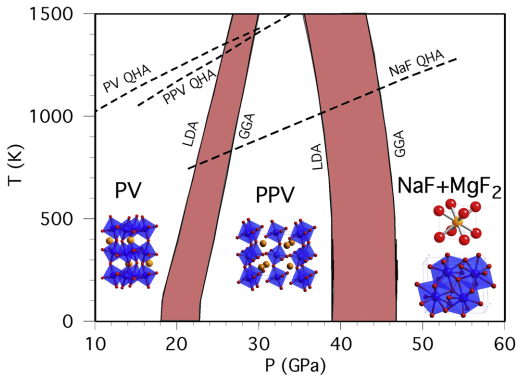

Figure 4. Calculated phase boundaries of $NaMgF_3$. NaF is CsCl-type and MgF_2 is cotunnite-type. Solid lines denote phase boundaries by LDA and GGA; real phase boundaries are expected to occur in red bands between them. Dashed lines represent the upper temperature limits in which QHA should be valid (see text); MgF_2's limit occurs over 1,500 K.

route to investigate properties of the PPV structure, including its dissociation.

[12] **Acknowledgments.** Calculations have been carried out using the Quantum-ESPRESSO package (http://www.pwscf.org). Research was supported by NSF grants EAR-0135533, EAR-0230319, EAR-0510501, and ITR-0428774 (VLab).

References

Baroni, S., S. de Gironcoli, A. Dal Corso, and P. Giannozzi (2001), Phonons and related crystal properties from density-functional perturbation theory, *Rev. Mod. Phys.*, *73*, 515.

Cortona, P. (1992), Direct determination of self-consistent total energies and charge densities of solids: A study of the cohesive properties of the alkali halides, *Phys. Rev. B*, *46*, 2008.

Giannozzi, P., S. de Gironcoli, P. Pavone, and S. Baroni (1991), Ab initio calculation of phonon dispersions in semiconductors, *Phys. Rev. B*, *43*, 7231.

Haines, J., J. M. Leger, F. Gorelli, D. D. Klug, J. S. Tse, and Z. Q. Li (2001), X-ray diffraction and theoretical studies of the high-pressure structures and phase transitions in magnesium fluoride, *Phys. Rev. B*, *64*, 134130.

Hyde, B. G., and S. Andersson (1989), *Inorganic Crystal Structures*, John Wiley, Hoboken, N. J.

Karki, B. B., R. M. Wentzcovitch, S. de Gironcoli, and S. Baroni (1999), First-principles determination of elastic anisotropy and wave velocities of MgO at lower mantle conditions, *Science*, *286*, 1705.

Liu, H.-Z., J. Chen, J. Hu, C. D. Martin, D. J. Weidner, D. Husermann, and H.-K. Mao (2005), Octahedral tilting evolution and phase transition in orthorhombic $NaMgF_3$ perovskite under pressure, *Geophys. Res. Lett.*, *32*, L04304, doi:10.1029/2004GL022068.

Murakami, M., K. Hirose, K. Kawamura, N. Sata, and Y. Ohishi (2004), Post-perovskite phase transition in $MgSiO_3$, *Science*, *304*, 855.

Oganov, A. R., and S. Ono (2004), Theoretical and experimental evidence for a post-perovskite phase of $MgSiO_3$ in Earth's D″ layer, *Nature*, *430*, 445.

Parise, J., K. Umemoto, R. M. Wentzcovitch, and D. Weidner (2004), Post-perovskite transition in $NaMgF_3$, *Eos Trans. AGU*, *85*(47), Fall Meet. Suppl., Abstract MR23A-0188.

Perdew, J. P., and A. Zunger (1981), Self-interaction correction to density-functional approximations for many-electron systems, *Phys. Rev. B*, *23*, 5048.

Perdew, J. P., K. Burke, and M. Ernzerhof (1996), Generalized gradient approximation made simple, *Phys. Rev. Lett.*, *77*, 3865.

Smith, R. W., W. N. Mei, J. W. Flocken, M. J. Dubik, and J. R. Hardy (2000), Polymorphic phase transitions in mixed alkali magnesium fluoride solid solutions, *Mater. Res. Bull.*, *35*, 341.

Tsuchiya, T., J. Tsuchiya, K. Umemoto, and R. M. Wentzcovitch (2004), Phase transition in $MgSiO_3$ perovskite in the Earth's lower mantle, *Earth Planet. Sci. Lett.*, *224*, 241.

Umemoto, K., R. M. Wentzcovitch, and P. B. Allen (2006), Dissociation of $MgSiO_3$ in the cores of gas giants and terrestrial exoplanets, *Science*, *311*, 983.

Vanderbilt, D. (1990), Soft self-consistent pseudopotentials in a generalized eigenvalue formalism, *Phys. Rev. B*, *41*, R7892.

Wallace, D. (1972), *Thermodynamics of Crystals*, John Wiley, Hoboken, N. J.

Wentzcovitch, R. M. (1991), Invariant molecular-dynamics approach to structural phase transitions, *Phys. Rev. B*, *44*, 2358.

Wentzcovitch, R. M., J. L. Martins, and G. D. Price (1993), Ab initio molecular dynamics with variable cell shape: Application to $MgSiO_3$, *Phys. Rev. Lett.*, *70*, 3947.

Wyckoff, R. W. G. (1965), *Crystal Structures*, vol. 2, Wiley-Interscience, Hoboken, N. J.

Yagi, T., T. Suzuki, and S. Akimoto (1983), New high-pressure polymorphs ion sodium halides, *J. Phys. Chem. Solids*, *44*, 135.

Zhao, Y., D. J. Weidner, J. B. Parise, and D. E. Cox (1993a), Thermal expansion and structural distortion of perovskite—Data for $NaMgF_3$ perovskite. Part I, *Phys. Earth Planet. Inter.*, *76*, 1.

Zhao, Y., D. J. Weidner, J. B. Parise, and D. E. Cox (1993b), Critical phenomena and phase transition of perovskite—Data for $NaMgF_3$ perovskite. Part II, *Phys. Earth Planet. Inter.*, *76*, 17.

Zhao, Y., et al. (1994), Perovskite at high P-T conditions: An in situ synchrotron X ray diffration study of $NaMgF_3$ perovskite, *J. Geophys. Res.*, *99*, 2871.

Zhou, L. X., J. R. Hardy, and H. Z. Cao (1997), Molecular dynamics simulation of superionicity in neighborite, $NaMgF_3$, *Geophys. Res. Lett.*, *24*, 747.

J. B. Parise and D. J. Weidner, Department of Earth and Space Sciences, State University of New York, Stony Brook, NY 11794-2100, USA.

K. Umemoto and R. M. Wentzcovitch, Minnesota Supercomputing Institute and Department of Chemical Engineering and Materials Science, University of Minnesota, Minneapolis, MN 55455, USA. (umemoto@cems.umn.edu)